

Analytical solutions for mechanical response of circular tunnels with double primary linings in squeezing grounds

Kui Wu^{1,2a}, Zhushan Shao^{*1}, Siyuan Hong^{1,2b} and Su Qin^{1,2c}

¹School of Civil Engineering, Xi'an University of Architecture and Technology, Xi'an 710055, China

²Shaanxi Ley Lab of Geotechnical and Underground Space Engineering (XAUAT), Xi'an University of Architecture and Technology, Xi'an 710055, China

(Received June 8, 2020, Revised July 30, 2020, Accepted August 18, 2020)

Abstract. Multi-layered primary linings have been proved to be highly effective for tunneling in severe squeezing grounds. But there still has not existed well-established design method for it. Basically, there are two main critical problems in this method, including determinations of allowable deformation and distribution of support stiffness. In order to address such problems, an attempt to investigate the mechanical response of a circular tunnel with double primary linings is performed in this paper. Analytical solutions in closed form for stresses and displacements around tunnels are derived. In addition, the effectiveness and reliability of theoretical formulas provided are well validated by using the numerical method. Finally, based on the analytical solutions, a parametric investigation on the effects of allowable deformation and distribution of support stiffness on tunnel performance is conducted. Results show that the rock pressure and displacement are significantly affected by these two design parameters. It can be found that rock pressure decreases as either allowable deformation increases or stiffness of the first primary lining decreases, but rock displacement shows an opposite trend. This paper can provide a useful guidance for the design of multi-layered primary linings.

Keywords: squeezing tunnel; double primary linings; analytical solution; parametric investigation

1. Introduction

With the rapid development of tunnelling technology, many tunnels have been successfully built in very complex geological conditions throughout the world (Kimura *et al.* 1987, Barla 2016, Niedbalski *et al.* 2018, Chen *et al.* 2019a, Sun *et al.* 2019, 2020, Tian *et al.* 2019, Wang *et al.* 2020, Wu *et al.* 2020a, Yuan *et al.* 2020). Especially, squeezing grounds are usually encountered by rock engineers during the whole tunnelling process, where time-dependent large deformations are prone to occur (Hu *et al.* 2019, 2020, Qiu *et al.* 2020, Liu *et al.* 2020). Overstressing of support caused by large deformations is still a big challenge for rock engineers to ensure the support structure safety and tunnel stability.

Basically, there are two main principles for tunnelling in squeezing grounds: the resistance principle and the yielding principle (Barla 2016). Heavy support system can be referred to as tunnel support structures following the resistance principle, where rock deformations are strictly restrained (Hoek 2001). Lessons learned from several unsuccessful cases in heavy support system have shown that the method of strengthening support structures may be

practically infeasible to address the problem of serious squeezing deformations because time-dependent deformations, reportedly, even contribute more than 70% of the total tunnel convergences in such geological conditions. Dalgıç (2002) pointed out that although the successful application of heavy support system was achieved in Bolu tunnel, the total thickness of primary lining and Bernold lining excluding the secondary lining had reached 1.0 m. Based on a better understanding of deformation mechanism of squeezing rocks, more and more attentions have moved to the yielding supports (Wu *et al.* 2020b). The idea behind the so-called “yielding supports” is that the rock pressure will decrease by allowing the ground to deform (Lackner *et al.* 2002, Barla 2016, Wu *et al.* 2020c). The yield in supports has been implemented by rock engineers in different ways. Cantieni and Anagnostou (2009) considered that the purpose of allowing rock to deform without support damage can be achieved through arranging a compressible layer between rock mass and stiff lining. Wu and Shao (2019a, b) have carried out analytical investigations on the influence of compressible layer on tunnel performance. Hoek and Guevara (2009) addressed the severe squeezing problems occurring in Yacambú-Quibor tunnel by the use of simple sliding joints in steel sets. Moritz (2011) discussed the mechanical properties of ductile tunnel linings based on yielding elements, and this type of support form was successfully applied in several projects, for instance Saint Martin La Porte access tunnel (Barla *et al.* 2011), Ceneri Base tunnel (Merlini *et al.* 2018) and Yangshan tunnel (Qiu *et al.* 2018). Multi-layered primary support, as one major type of yielding supports, has been well recognized as one

*Corresponding author, Professor, Ph.D.

E-mail: shaozhushan@xauat.edu.cn

^aPh.D. Student

^bMaster Student

^cPh.D. Student

effective method to address serious squeezing deformation problems (Chen *et al.* 2019b). However, it has to be admitted that there are still two main critical problems in this method. Herein, only double primary linings is discussed. One is the supporting opportunity of the second primary lining (also can be referred to as allowable deformation of the first primary lining), and the other is the distribution of stiffnesses of the first and second primary linings.

Analytical method should be able to provide a possible approach to address such problems. As well known, stresses and displacements around tunnels can be effectively predicted by using analytical solutions (Tian *et al.* 2020). Furthermore, a better understanding of how final solutions are influenced by parameters involved could be obtained. Many elastic or elastic-plastic solutions for stresses and displacements have been available in many literatures (Hefny and Lo 1999, Bobet 2001, Exadaktylos and Stavropoulou 2002, Kargaret *et al.* 2014). Considering the time-dependent properties of squeezing rocks (Malan 2002, Paraskevopoulou and Diederichs 2018), some time-dependent solutions are also provided by some researchers (Sulem *et al.* 1987, Nomikos *et al.* 2011, Brichall and Osman 2012, Song *et al.* 2018a, b, Chu *et al.* 2019, 2020a, b). However, it can be found that although a variety of factors were taken into account in literatures above, analytical solutions for stresses and displacements around tunnels with multi-layered primary supports have never been available.

In this study, a theoretical investigation into the mechanical response of a lined circular tunnel with double primary linings in squeezing rocks is carried out. The squeezing behavior of rocks is described by the viscoelastic Burgers model. Analytical solutions in closed form for stresses and displacements around tunnels are derived. Then, the effectiveness and reliability of theoretical formulas provided are well validated by using the numerical method. Finally, based on the analytical solutions, a parametric investigation on the effects of allowable deformation and distribution of support stiffness on tunnel performance is conducted.

2. Problem definition and assumptions

This paper involves a lined circular tunnel with double primary linings in squeezing rocks. The tunnel is driven at such a great depth compared with its dimension that the tunnel can be assumed to be an axisymmetric hole, subjected to a uniform stress state at infinity (Kargaret *et al.* 2014). The rock medium is isotropic and homogeneous, which time-dependent squeezing behavior can be described by viscoelastic Burgers model (Nomikos *et al.* 2011, Brichall and Osman 2012, Chu *et al.* 2019, Wu *et al.* 2020d). Primary support is characterized by linear-elastic response under loading without failure. In this paper, mechanical response of a circular tunnel with double primary linings is discussed.

The Burgers model is coupled in series by a Maxwell unit and Kelvin element, as presented in Fig. 1. Maxwell unit is formed by a linear elastic spring and a linear dashpot

connected in series. Under a constant stress immediately, the Maxwell model displays an elastic instantaneous strain firstly followed by a steadily increasing and irreversible creep behavior. The constitutive equation of Maxwell can be expressed as Eq. (1). Kelvin model consists of a linear elastic spring and a linear dashpot connected in parallel. Once by an instantly applied load, the strain in Kelvin model increases asymptotically to its final value. The constitutive equation of Kelvin model takes the form in Eq. (2).

$$\dot{e}_{ij}^M = \frac{s_{ij}^M}{2\eta^M} + \frac{\dot{s}_{ij}^M}{2G^M} \quad (1)$$

in which the overdot denotes the time derivative. The superscript M is the components of the corresponding variables in the Maxwell unit. s_{ij} and e_{ij} represent the tensors of stress and strain deviators, respectively. G and η denote the spring constant and viscosity coefficient of dashpot, respectively.

$$s_{ij}^K = 2G^K e_{ij}^K + 2\eta^K \dot{e}_{ij}^K \quad (2)$$

where the superscript K denotes the components of the corresponding variables in the Kelvin element.

Goodman (1989) pointed out that for many practical purposes Burgers model was preferable, because only four unknown parameters were involved in this model and different deforming stages of rocks, including elastic strain, decay creep and steady creep, could be well displayed by using Burgers model. The deforming curve of Burgers model under the constant stress is presented in Fig. 2. For Burgers model, the constitutive equation can be given by

$$\begin{cases} s_{ij} = s_{ij}^M = s_{ij}^K \\ e_{ij} = e_{ij}^K + e_{ij}^M \end{cases} \quad (3)$$

By substituting Eqs. (1) and (2) into Eq. (3), Eq. (3) can be rewritten as

$$\begin{aligned} \ddot{s}_{ij} + \left(\frac{G^M}{\eta^M} + \frac{G^M}{\eta^K} + \frac{G^K}{\eta^K} \right) \dot{s}_{ij} + \left(\frac{G^M G^K}{\eta^M \eta^K} \right) s_{ij} \\ = 2G^M \ddot{e}_{ij} + 2 \frac{G^M G^K}{\eta^K} \dot{e}_{ij} \end{aligned} \quad (4)$$

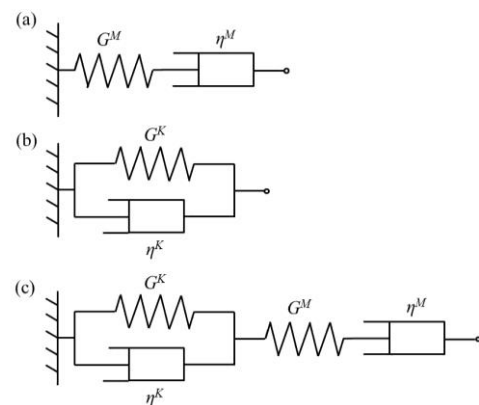


Fig. 1 Physical model (a) Maxwell model, (b) Kelvin model and (c) Burgers model

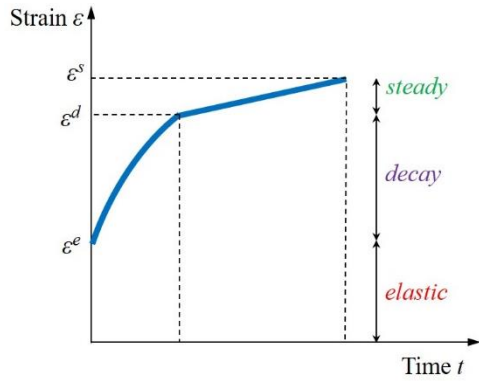


Fig. 2 Curve for creep behavior of Burgers model

 Table 1 Coefficients of A_k and B_k in Burgers model

k	2	1	0
A_k	1	$G^M/\eta^{M+1} + G^M/\eta^k + G^k/\eta^k$	$G^M G^k/\eta^M \eta^k$
B_k	$2G^M$	$2G^M G^k/\eta^k$	0

For simplifying the above differential equation, the linear differential time operators Q and P are employed, which are given by

$$P = \sum_0^2 A_k \frac{d^k}{dt^k}, \quad Q = \sum_0^2 B_k \frac{d^k}{dt^k} \quad (5)$$

in which A_k and B_k are listed in Table 1.

Thus the Eq. (4) can be re-expressed as

$$P S_{ij} = Q e_{ij} \quad (6)$$

Furthermore, Eq. (6) in r, θ, z becomes in cylindrical coordinates

$$P(\sigma_r - \sigma_{mean}) = Q(\varepsilon_r - \varepsilon_{mean}) \quad (7)$$

$$P(\sigma_\theta - \sigma_{mean}) = Q(\varepsilon_\theta - \varepsilon_{mean}) \quad (8)$$

$$P(\sigma_z - \sigma_{mean}) = Q(\varepsilon_z - \varepsilon_{mean}) \quad (9)$$

In the equation, the stress and strain components are functions of r, θ and z , respectively. σ_{mean} and ε_{mean} denote the mean stress and strain, respectively, calculated as

$$\begin{cases} \sigma_{mean} = \frac{\sigma_r + \sigma_\theta + \sigma_z}{3} \\ \varepsilon_{mean} = \frac{\varepsilon_r + \varepsilon_\theta + \varepsilon_z}{3} \end{cases} \quad (10)$$

3. Prediction for stresses and displacements

3.1 Fundamental formula

As previously mentioned, the lined circular tunnel can be considered as a hole, which is subjected to the hydrostatic pressure. The mechanical model of the lined

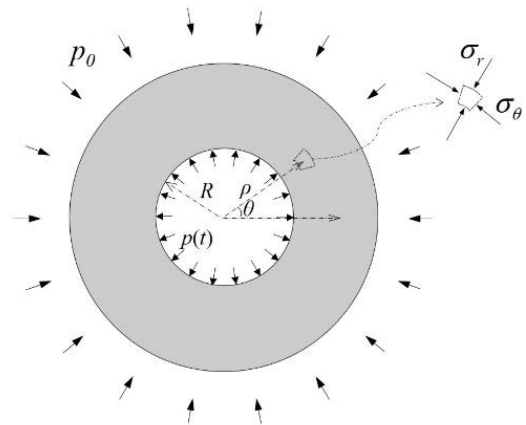


Fig. 3 Mechanical model of pressure hole

tunnel is presented in Fig. 3. Based on the elastic-viscoelastic correspondence principle, the stress field can be written as

$$\begin{cases} \sigma_{rr} = \left(1 - \frac{R^2}{\rho^2}\right) p_0 + \frac{R^2}{\rho^2} p(t) \\ \sigma_{\theta\theta} = \left(1 + \frac{R^2}{\rho^2}\right) p_0 - \frac{R^2}{\rho^2} p(t) \end{cases} \quad (11)$$

in which p_0 represents the uniform stress and $p(t)$ is the internal pressure. R and ρ denote the hole radius and distance between element and hole center, respectively.

Then, the deviatoric stress field of this mechanical model can be calculated as from the Eq. (11).

$$\begin{cases} \Delta\sigma_{rr} = [-p_0 + p(t)] \frac{R^2}{\rho^2} \\ \Delta\sigma_{\theta\theta} = [p_0 - p(t)] \frac{R^2}{\rho^2} \end{cases} \quad (12)$$

where $\Delta\sigma_{rr}$ and $\Delta\sigma_{\theta\theta}$ are the radial and tangential deviatoric stresses, respectively.

By substituting $\rho=R$ into the Eq. (12) the deviatoric stress at the hole wall can be given by

$$\begin{cases} \Delta\sigma_{rr} = -p_0 + p(t) \\ \Delta\sigma_{\theta\theta} = p_0 - p(t) \end{cases} \quad (13)$$

Based on the displacement-strain relation, the tangential strain difference can be calculated as the Eq. (14) in the form of displacement.

$$\Delta\varepsilon_{\theta\theta} = u(r, t) / r \quad (14)$$

in the equation, $\Delta\varepsilon_{\theta\theta}$ represents the tangential deviatoric strain and $u(r, t)$ is radial displacement.

Thus, on the hole wall, i.e., $r=R$, the Eq. (14) becomes

$$\Delta\varepsilon_{\theta\theta} = u_R(t) / R \quad (15)$$

where $u_R(t)$ is the radial displacement at the hole wall.

According to the assumptions above, the response of a lined circular tunnel with the double primary linings is

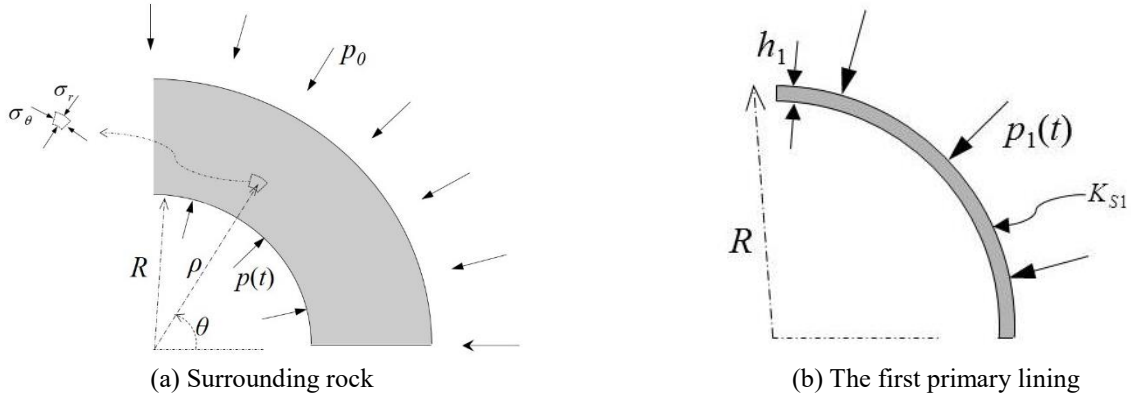


Fig. 4 Mechanical model of tunnel

investigated in the following section. The first primary lining with weak stiffness is applied immediately after the tunnel excavation completed. As the tunnel displacement under the circumstance of the first primary lining reaches a predetermined value u_0 at time $t=t_0$, the installation of the second primary lining with high stiffness follows.

3.2 Analytical prediction at the first stage

Fig. 4 illustrates the 1/4 mechanical model for interaction between surrounding rock and the first primary lining. In Fig. 4, $p_1(t)$ is the interaction force between the surrounding rock and the first primary lining. As shown in Fig. 4(a), the model of surrounding rock can be considered as a pressure hole, with the interaction force $p_1(t)$ being the internal pressure.

Because the first primary lining is constructed after the underground excavation finished, the pressure $p_1(t)$ induced by rock time-dependent deformation can be given by

$$p_1(t) = K_{S1} \frac{u_R(t) - u_R(0)}{R} \quad (16)$$

in which K_{S1} represents the stiffness of the first primary lining and $u_R(0)$ is the instantaneous radial displacement at the tunnel wall after excavation.

Substituting Eq. (16) into Eq. (13) provides the tangential deviatoric stress at the tunnel wall as

$$\Delta\sigma_{\theta\theta} = p_0 - K_{S1} \frac{u_R(t) - u_R(0)}{R} \quad (17)$$

Thus the displacement governing equation in the surrounding rock/first primary lining interface can be expressed by substituting the Eqs. (15) and (17) in to Eq. (8) as follows

$$\sum_0^2 (B_k + K_{S1}A_k) \frac{d^k}{dt^k} u_R(t) = A_0 [K_{S1}u_R(0) + p_0R] \quad (18)$$

Remarkably, the Eq. (18) is a linear second-order differential equation in the form of $u_R(t)$ and thus two initial boundary conditions are required to obtain the analytical solution for displacement through solving the Eq. (18). The first should be the instantaneous radial displacement after tunnel excavation completed at time $t=0$. Based on the

property of Burgers model and geometric parameters of tunnel, it can be calculated as

$$u_R(0) = \frac{p_0R}{2G^M} \quad (19)$$

From the installation of the first primary lining, the coordinate deformation in the surrounding rock/first primary lining interface needs to be achieved. The other initial boundary condition should be the displacement rate at time $t=0$, being computed as

$$\dot{u}_R(0) = \frac{p_0R}{2(1 + K_{S1}/2G^M)} \left(\frac{1}{\eta^M} + \frac{1}{\eta^K} \right) \quad (20)$$

Using the Eqs. (19) and (20) the tunnel displacement of the Eq. (18) at the first stage could be solved as

$$u_R(t) = \frac{p_0R}{K_{S1}} \left[\left(\frac{K_{S1}}{2G^M} + 1 \right) + \frac{F_1 e^{a_1 t} - F_2 e^{a_2 t}}{a_1 - a_2} \right] \quad (21)$$

with $a_{1,2}$ being the roots (both negative) of the following quadratic equation:

$$a^2 + \left[\frac{2G^M / K_{S1} + G^M / G^K + T^K / T^M + 1}{(2G^M / K_{S1} + 1)T^K} \right] a + \left[\frac{1}{(2G^M / K_{S1} + 1)T^K T^M} \right] = 0 \quad (22)$$

and F_1, F_2 are given by:

$$F_1 = \frac{1 + a_1 T^K (1 + \eta^M / \eta^K)}{a_1 (2G^M / K_{S1} + 1) T^K T^M} \quad (23)$$

$$F_2 = \frac{1 + a_2 T^K (1 + \eta^M / \eta^K)}{a_2 (2G^M / K_{S1} + 1) T^K T^M} \quad (24)$$

Then substituting the Eq. (21) into Eq. (16) provides the analytical solution for $p_1(t)$ as follows

$$p_1(t) = p_0 \left(1 + \frac{F_1 e^{a_1 t} - F_2 e^{a_2 t}}{a_1 - a_2} \right) \quad (25)$$

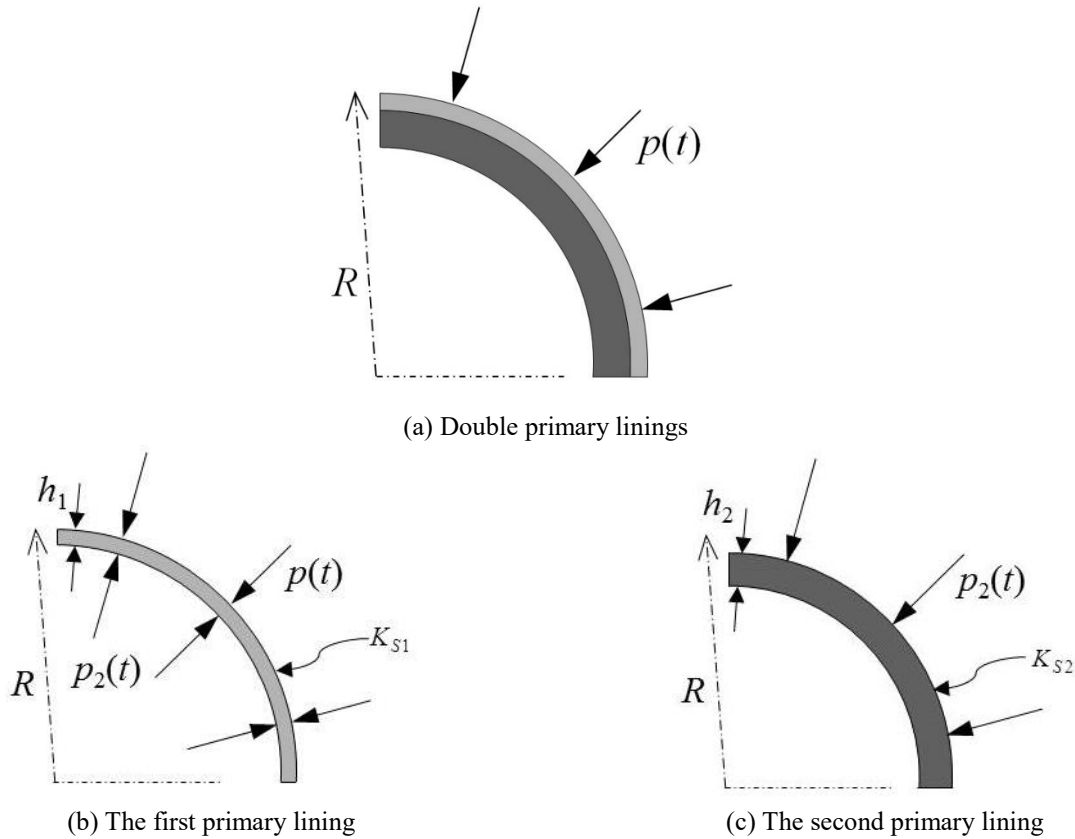


Fig. 5 Mechanical model of double primary linings at second stage

3.3 Analytical prediction at the second stage

When the tunnel displacement reaches a predetermined value u_0 at time $t=t_0$, in other words, the rock deformation has been released to some extent, the second primary lining with higher stiffness needs to be installed promptly to keep the tunnel stability. After the installation of the second primary lining, two primary linings work together to resist the time-dependent deformations of surrounding rock (See Fig. 5). The rock pressure acting on the two primary linings can be referred as $p(t)$, and the loads undertaken by the first primary lining and second primary lining are as $p_1(t)$ and $p_2(t)$ respectively, where $p_1(t)$ can be calculated by $p(t)-p_2(t)$.

From time $t= t_0$, the load acting on the second primary lining $p_2(t)$ can be written as

$$p_2(t) = K_{S2} \frac{u_R(t) - u_R(t_0)}{R} \quad (26)$$

where K_{S2} denotes the stiffness of the second primary lining.

Substituting the Eqs. (16) and (26) into Eq. (13) provides the tangential stress in the surrounding rock/primary support interface as

$$\Delta\sigma_{\theta\theta} = p_0 - K_{S1} \frac{u_R(t) - u_R(0)}{R} - K_{S2} \frac{u_R(t) - u_R(t_0)}{R} \quad (27)$$

Then by substituting the Eqs. (15) and (27) into Eq. (8), the following displacement equation can be given by

$$\sum_0^2 (B_k + A_k K_{S1} + A_k K_{S2}) \frac{d^k}{dt^k} u_R(t) = A_0 [p_0 R + K_{S1} u_R(0) + K_{S2} u_R(t_0)] \quad (28)$$

Similarly, two initial conditions are also required in order to obtain the solution of the equation (28). Based on the Eq. (21), the initial displacement at time $t=t_0$, could be expressed as

$$u_R(t_0) = u_0 = \frac{p_0 R}{K_{S1}} \left[\left(\frac{K_{S1}}{2G^M} + 1 \right) + \frac{F_1 e^{a_1 t_0} - F_2 e^{a_2 t_0}}{a_1 - a_2} \right] \quad (29)$$

Since the installation of the second primary lining with higher stiffness at time $t=t_0$, the increase of contact surfaces results in the complexity of theoretical analyses. Two coordination conditions in the surrounding rock/first primary lining interface and the first primary lining/second primary lining interface should be met at the same time. Based on the analyses of tunnel deformation, the initial displacement rate at time $t=t_0$ could be expressed as

$$\dot{u}_R(t_0) = \frac{p_0 R (F_1 a_1 e^{a_1 t_0} - F_2 a_2 e^{a_2 t_0})}{K_{S1} (1 + K_{S2} / 2G^M) (a_1 - a_2)} \quad (30)$$

By use of the Eqs. (29) and (30), the analytical solution for tunnel displacement after the installation of the second primary lining can be calculated as

$$u_r(t) = p_0 R \left[\frac{1 + K_{S1} / 2G^M + K_{S2} u_0 / p_0 R}{K_{S1} + K_{S2}} + \frac{F_3 e^{a_3(t-t_0)} - F_4 e^{a_4(t-t_0)}}{a_3 - a_4} \right] \quad (31)$$

with $a_{3,4}$ being the roots (both negative) of the following equation:

$$a^2 + \left[\frac{2G^M / (K_{S1} + K_{S2}) + G^M / G^K + T^K / T^M + 1}{[2G^M / (K_{S1} + K_{S2}) + 1] T^K} \right] a + \left[\frac{1}{[2G^M / (K_{S1} + K_{S2}) + 1] T^K T^M} \right] = 0 \quad (32)$$

and F_3, F_4 are given by

$$F_3 = a_4 \left[\frac{1 + K_{S1} / 2G^M + K_{S2} u_0 / p_0 R}{K_{S1} + K_{S2}} - \frac{u_0}{p_0 R} \right] + \frac{F_1 a_1 e^{a_1 t_0} - F_2 a_2 e^{a_2 t_0}}{K_{S1} (1 + K_{S2} / 2G^M) (a_1 - a_2)} \quad (33)$$

$$F_4 = a_3 \left[\frac{1 + K_{S1} / 2G^M + K_{S2} u_0 / p_0 R}{K_{S1} + K_{S2}} - \frac{u_0}{p_0 R} \right] + \frac{F_1 a_1 e^{a_1 t_0} - F_2 a_2 e^{a_2 t_0}}{K_{S1} (1 + K_{S2} / 2G^M) (a_1 - a_2)} \quad (34)$$

Based on the Eqs. (16), (26) and (31), the pressures acting on the first and second primary linings from time $t=t_0$ can be expressed as follows, respectively.

$$p_1(t) = p_0 K_{S1} \left[\frac{1 + K_{S1} / 2G^M + K_{S2} u_0 / p_0 R}{K_{S1} + K_{S2}} + \frac{F_3 e^{a_3(t-t_0)} - F_4 e^{a_4(t-t_0)}}{a_3 - a_4} - \frac{1}{2G^M} \right] \quad (35)$$

$$p_2(t) = p_0 K_{S2} \left[\frac{1 + K_{S1} / 2G^M + K_{S2} u_0 / p_0 R}{K_{S1} + K_{S2}} + \frac{F_3 e^{a_3(t-t_0)} - F_4 e^{a_4(t-t_0)}}{a_3 - a_4} - \left(\frac{1}{2G^M} + \frac{1}{K_{S1}} \right) - \frac{F_1 e^{a_1 t_0} - F_2 e^{a_2 t_0}}{K_{S1} (a_1 - a_2)} \right] \quad (36)$$

4. Results and discussion

4.1 Verification

In order to ensure the reliability and effectiveness of the theoretical analyses, numerical calculation using finite element software Abaqus is carried out in this section. The detailed information of the numerical model is shown in Fig. 6. Notably, the tunnel radius, initial ground stress, rock

Table 2 Calculation parameters

Geometry and loading			
Tunnel radius R /m		Initial ground stress p_0 /MPa	
4.572		6.895	
Rock parameters			
G^K /MPa	η^K /MPa·year	G^M /MPa	η^M /MPa·year
344.738	655.758	3447.379	131183.409
Support properties			
E /MPa	ν	K_{S1} /MPa	K_{S2} /MPa
16547.42	0.2	508.4	2033.6

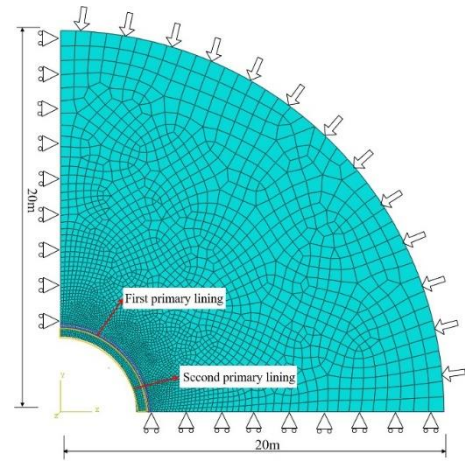


Fig. 6 Illustration for numerical model

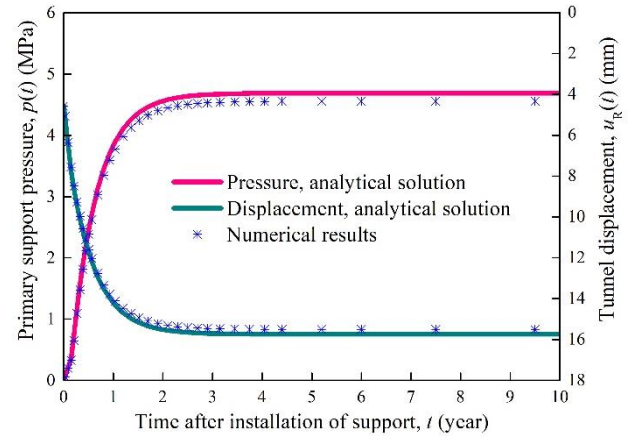


Fig. 7 The curves of displacement and pressure in the condition of $u_0=8$ mm

parameters and support properties employed in this numerical calculation are all derived from Goodman (1989) and listed in Table 2. In order to numerically simulate the case of double primary linings in tunnel, the stiffness of lining in Goodman's study is divided into two parts according to the ratio of 2:8, and these two values of stiffness are assigned to the first primary lining and second primary lining, respectively. In addition, the installation of the second primary lining is placed with the predetermined value u_0 reaching 8 mm.

As shown in Fig. 7, curves for pressure and

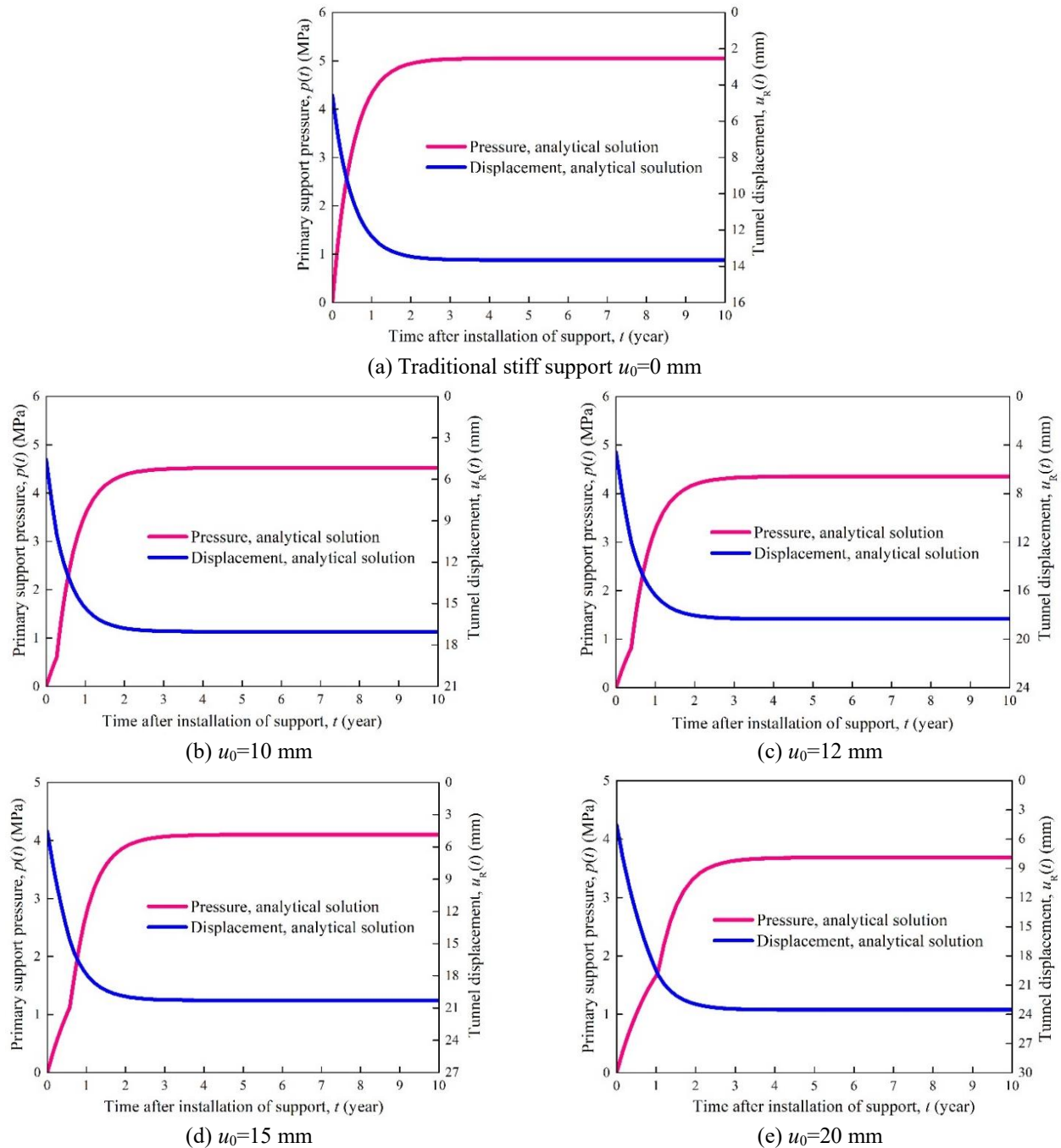


Fig. 8 The curves of displacement and pressure versus time

displacement by use of analytical solutions and numerical results are plotted, respectively. A good agreement between them exhibits the effectiveness and reliability of theoretical analyses. It can be seen from the pressure curve in Fig. 7 that there exists a change of slope at time approximately $t_0=1$ month, which implies the placement of the second primary lining. It is safe to conclude that the installation time of the second primary lining and the distribution of stiffnesses of the two primary linings can pose a great influence on the calculation results.

4.2 Parametric investigation

Design of the tunnel support structures is usually

constructed based on an understanding of the influence of different parameters involved. For double primary linings, the predetermined deformation value u_0 is one of the very important parameters. According to the above theoretical formulas, the investigation on the effect of predetermined value u_0 on the displacement and pressure is performed. As illustrated in Fig. 8, curves for displacement and pressure with different predetermined values u_0 are plotted, which are drawn for $u_0=0, 10, 12, 15, 20$ mm. Notably, when the value u_0 is equal to zero, it means the double primary linings becomes the traditional stiff support again.

As shown in Figs. 7 and 8, the predetermined deformation value u_0 has a great influence on pressure and

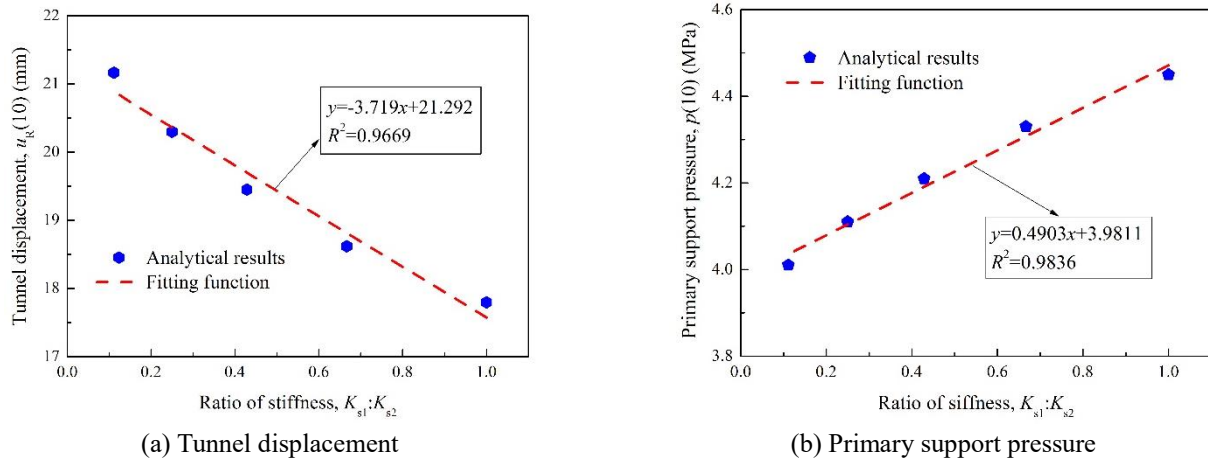


Fig. 9 Curves for tunnel displacement and primary support pressure under different stiffness ratios

displacement. Generally, the pressure and displacement in above cases all present a same development law, which should be closely associated with rock rheological properties. Their evolution trend could be divided into three stages, quickly increasing stage, slowly increasing stage and steady stage. In addition, it could be found that the pressure acting on the primary support decreases and displacement increases with the increase of predetermined deformation value u_0 . This is because a great release of rock deformation can be achieved as value u_0 increases.

Further, in the diagrams of Figs. 7 and 8, the pressures with different predetermined values u_0 at $t=10$ year calculated by closed form solutions hold about 5.05 MPa, 4.69 MPa, 4.52 MPa, 4.35 MPa, 4.10 MPa and 3.68 MPa, respectively. In order to better show the effect of u_0 on pressure, the pressure under traditional stiff support ($u_0=0$) is selected as a reference. It could be found that compared with traditional stiff support, pressure acting on the double primary linings are reduced by 7.78%, 11.79%, 16.08%, 23.24% and 37.23%, respectively. It could be concluded that it is feasible to improve the support stress condition by the use of double primary linings. However, this is also never the case that larger u_0 indicates better supporting effect. It is obvious that, if the predetermined value u_0 is designed too large, pressure on the first primary lining with weak stiffness would exceed its bearing capacity and it may fail to work before the installation of the second primary lining. Then, the theoretical analyses provided in this paper may be not applicable any more.

Results above also show that tunnel displacement continues to increase with the predetermined deformation value u_0 , which is unexpected in the practical engineering. However, it is useful to use the solutions in this paper in order to evaluate the final deformation in the design stage and then combine a certain amount of over-excavation to accommodate the deformation in tunneling construction, which would not cause exceeding clearance limit of support and threaten safety of tunnel.

The distribution of stiffnesses of double primary linings is one of the main problems confusing rock engineers and its effect on the pressure and displacement is here also studied. As shown in Fig. 9, these diagrams are drawn for the predetermined deformation value $u_0=15$ mm. Five cases of

ratios of the first primary lining stiffness to second lining stiffness are 1:9, 2:8, 3:7, 4:6, 5:5, respectively.

In the diagrams of Fig. 9, the variations of primary support pressure and tunnel displacement at time $t=10$ year under different cases are shown. From Fig. 9, in the linearly viscoelastic rocks, the primary support pressure presents a linearly increasing trend and tunnel displacement decreases linearly with ratios of stiffness. Results in Fig. 9 show that although under the same predetermined deformation value u_0 , the primary support pressure decreases with reduction of stiffness of the first primary lining, which also validates the advantages of double primary linings. However, the first primary lining with weaker stiffness would bring about greater displacement. As mentioned before, such problem could be addressed by over-excavation according to the calculation results.

Remarkably, in order to effectively release the rock deformation and make the first primary lining co-deform with surrounding rock, it does not imply that stiffness of the first primary lining should be as small as possible. Because of the low strength and weak self-stabilization of squeezing rock, there would be a high risk of tunnel instability after excavation finished. Rock engineers need to promptly provide strong resistance force to guarantee the rock instability, which requires the first primary lining with sufficient stiffness. In sum, the determination of optimal stiffness of two primary linings in practical engineering involves a comprehensive investigation combining rock properties and tunnel design requirements.

5. Conclusions

Multi-layered primary linings have been proved to be highly effective for tunneling in severe squeezing grounds. But there still has not existed well-established design method for it. Basically, there are two main critical problems in this method, including determinations of allowable deformation and distribution of support stiffness. In this study, focusing on the design of double primary linings in squeezing tunnels, viscoelastic solutions in closed form for stresses and displacements around tunnels with double primary linings are derived. The following

conclusions are drawn from this study:

In tunnels supported by double primary linings, where the time-dependent behavior of rock represented by Burgers model, the evolution trend of rock pressure and displacement could be divided into three stages, quickly increasing stage, slowly increasing stage and steady stage.

Rock pressure and tunnel displacement are significantly influenced by the allowable deformation described by predetermined deformation value in this study. It could be found that compared with traditional stiff support the rock pressure are reduced by 7.78%, 11.79%, 16.08%, 23.24% and 37.23% with $u_0=0, 10, 12, 15, 20$ mm, respectively. However, tunnel displacement gradually increases with the increase of this value.

The distribution of stiffnesses of double primary linings is one of the most important parameters for tunnel performance. Under the same predetermined deformation value, the primary support pressure presents a linearly increasing trend and tunnel displacement decreases linearly with ratios of stiffness in the linearly viscoelastic rock. However, this does not imply that stiffness of the first primary lining can be as small as possible. Because there would be a high risk of rock instability after excavation completed, the first primary lining also should provide sufficient and prompt supporting force to keep the stability of surrounding rock before the installation of the second primary lining.

Acknowledgments

The authors wish to acknowledge the funding for this research from the National Natural Science Foundation of China (No. 11872287) and the Found of Shaanxi Key Research Project (No. 2019ZDLGY01-10).

References

- Barla, G. (2016), "Full-face excavation of large tunnels in difficult conditions", *J. Rock Mech. Geotech. Eng.*, **8**(3), 294-303. <https://doi.org/10.1016/j.jrmge.2015.12.003>.
- Barla, G., Bonini, M. and Semeraro, M. (2011), "Analysis of the behaviour of a yield-control support system in squeezing rock", *Tunn. Undergr. Sp. Tech.*, **26**(1), 146-154. <https://doi.org/10.1016/j.tust.2010.08.001>.
- Bobet, A. (2001), "Analytical solutions for shallow tunnels in saturated ground", *J. Eng. Mech.*, **127**(12), 1258-1266. [https://doi.org/10.1061/\(ASCE\)0733-9399\(2001\)127:12\(1258\)](https://doi.org/10.1061/(ASCE)0733-9399(2001)127:12(1258)).
- Brichall, T.J. and Osman, A.S. (2012), "Response of a tunnel deeply embedded in a viscoelastic medium", *Int. J. Numer. Anal. Meth. Geomech.*, **36**(15), 1717-1740. <https://doi.org/10.1002/nag.1069>.
- Cantieni, L. and Anagnostou, G. (2009), "The interaction between yielding supports and squeezing ground", *Tunn. Undergr. Sp. Tech.*, **24**(3), 309-322. <https://doi.org/10.1016/j.tust.2008.10.001>.
- Chen, T., Feng, X.T., Cui, G., Tan, Y. and Pan, Z. (2019a), "Experimental study of permeability change of organic-rich gas shales under high effective stress", *J. Nat. Gas Sci. Eng.*, **64**, 1-14. <https://doi.org/10.1016/j.jngse.2019.01.014>.
- Chen, Z., He, C., Xu, G., Ma, G. and Yang, W. (2019b), "Supporting mechanism and mechanical behavior of a double primary support method for tunnels in broken phyllite under high geo-stress: A case study", *B. Eng. Geol. Environ.*, **78**(7), 5253-5267. <https://doi.org/10.1007/s10064-019-01479-1>.
- Chu, Z., Wu, Z., Liu, B. and Liu, Q. (2019), "Coupled analytical solutions for deep-buried circular lined tunnels considering tunnel face advancement and soft rock rheology effects", *Tunn. Undergr. Sp. Tech.*, **94**, 103111. <https://doi.org/10.1016/j.tust.2019.103111>.
- Chu, Z., Wu, Z., Liu, Q. and Liu, B. (2020a), "Analytical solutions for deep-buried lined tunnels considering longitudinal discontinuous excavation in rheological rock mass", *J. Eng. Mech.*, **146**(6), 04020047. [https://doi.org/10.1061/\(ASCE\)EM.1943-7889.0001784](https://doi.org/10.1061/(ASCE)EM.1943-7889.0001784).
- Chu, Z., Wu, Z., Liu, Q. and Liu, B. (2020b), "Analytical solution for lined circular tunnels in deep viscoelastic Burgers rock considering the longitudinal discontinuous excavation and sequential installation of liners", *J. Eng. Mech.*, **147**(1), In Press.
- Dalgıç, S. (2002), "Tunneling in squeezing rock, the Bolu tunnel, Anatolian Motorway, Turkey", *Eng. Geol.*, **67**(1-2), 73-96. [https://doi.org/10.1016/S0013-7952\(02\)00146-1](https://doi.org/10.1016/S0013-7952(02)00146-1).
- Exadaktylos, G.E. and Stavropoulou, M.C. (2002), "A closed-form elastic solution for stresses and displacements around tunnels", *Int. J. Rock Mech. Min. Sci.*, **39**(7), 905-916. [https://doi.org/10.1016/S1365-1609\(02\)00079-5](https://doi.org/10.1016/S1365-1609(02)00079-5).
- Goodman, R.E. (1989), *Introduction to Rock Mechanics*, 2th Edition, Wiley, New York, U.S.A.
- Hefny, A.M. and Lo, K.Y. (1999), "Analytical solutions for stresses and displacements around tunnels driven in cross-anisotropic rocks", *Int. J. Numer. Anal. Meth. Eng.*, **23**(2), 161-177. [https://doi.org/10.1002/\(SICI\)10969853\(199902\)23:2<161::AID-NAG963>3.0.CO;2-B](https://doi.org/10.1002/(SICI)10969853(199902)23:2<161::AID-NAG963>3.0.CO;2-B).
- Hoek, E. (2001), "Big tunnels in bad rock", *J. Geotech. Geoenviron. Eng.*, **127**(9), 726-740. [https://doi.org/10.1061/\(ASCE\)1090-0241\(2001\)127:9\(726\)](https://doi.org/10.1061/(ASCE)1090-0241(2001)127:9(726)).
- Hoek, E. and Guevara, R. (2009), "Overcoming squeezing in the Yacambú-Quibor tunnel, Venezuela", *Rock Mech. Rock Eng.*, **42**(2), 389-418. <https://doi.org/10.1007/s00603-009-0175-5>.
- Hu, B., Sharifzadeh, M., Feng, X.T., Talebi, R. and Lou, J.F. (2020), "Ground support performance in deep underground mine with large anisotropic deformation using calibrated numerical simulation (case of mine-H)", *Geomech. Eng.*, **21**(6), 551-564. <https://doi.org/10.12989/gae.2020.21.6.551>.
- Hu, B., Yang, S.Q. and Tian, W.L. (2019), "Creep-permeability behavior of sandstone considering thermal-damage", *Geomech. Eng.*, **18**(1), 71-83. <https://doi.org/10.12989/gae.2019.18.1.071>.
- Kargar, A.R., Rahmamejad, R. and Hajabasi, M.A. (2014), "A semi-analytical elastic solution for stress field of lined non-circular tunnels at great depth using complex variable method", *Int. J. Solids Struct.*, **51**(6), 1475-1482. <https://doi.org/10.1016/j.ijsolstr.2013.12.038>.
- Kimura, F., Okabayashi, N. and Kawamoto, T. (1987), "Tunnelling through squeezing rock in two large fault zones of the Enasan Tunnel II", *Rock Mech. Rock Eng.*, **20**(3), 151-166. <https://doi.org/10.1007/BF01020366>.
- Lackner, R., Macht, J., Hellmich, C. and Mang, H.A. (2002), "Hybrid method for analysis of segmented shotcrete tunnel linings", *J. Geotech. Geoenviron. Eng.*, **128**(4), 298-308. [https://doi.org/10.1061/\(ASCE\)1090-0241\(2002\)128:4\(298\)](https://doi.org/10.1061/(ASCE)1090-0241(2002)128:4(298)).
- Liu, T., Xie, Y., Feng, Z., Luo, Y., Wang, K. and Xu, W. (2020), "Better understanding the failure modes of tunnels excavated in the boulder-cobble mixed strata by distinct element method", *Eng. Fail. Anal.*, **116**, 104712. <https://doi.org/10.1016/j.engfailanal.2020.104712>.
- Malan, D.F. (2002), "Simulating the time-dependent behavior of

- excavations in hard rock”, *Rock Mech. Rock Eng.*, **35**(4), 225-254. <https://doi.org/10.1007/s00603-002-0026-0>.
- Merlini, D., Stocker, D., Falanesca, M. and Schuerch, R. (2018), “The Ceneri base tunnel: Construction experience with the southern portion of the flat railway line crossing the Swiss Alps”, *Engineering*, **4**(2), 235-248. <https://doi.org/10.1016/j.eng.2017.09.004>.
- Moritz, B. (2011), “Yielding elements—requirements, overview and comparison”, *Geomech. Tunn.*, **4**(3), 221-236. <https://doi.org/10.1002/geot.201100014>.
- Niedbalski, Z., Malkowski, P. and Majcherczyk, T. (2018), “Application of the NATM method in the road tunneling works in difficult geological conditions-The Carpathian flysch”, *Tunn. Undergr. Sp. Tech.*, **74**, 41-59. <https://doi.org/10.1016/j.tust.2018.01.003>.
- Nomikos, P., Rahmannedjad, R. and Sofianos, A. (2011), “Supported axisymmetric tunnels within linear viscoelastic Burgers rocks”, *Rock Mech. Rock Eng.*, **44**(5), 553-564. <https://doi.org/10.1007/s00603-011-0159-0>.
- Paraskevopoulou, C. and Diederichs, M. (2018), “Analysis of time-dependent deformation in tunnels using the convergence-confinement method”, *Tunn. Undergr. Sp. Tech.*, **71**, 62-80. <https://doi.org/10.1016/j.tust.2017.07.001>.
- Qiu, J., Lu, Y., Lai, J., Zhang, Y., Yang, T. and Wang, K. (2020), “Experimental study on the effect of water gushing on loess metro tunnel”, *Environ. Earth Sci.*, **79**, 261. <https://doi.org/10.1007/s12665-020-08995-4>.
- Qiu, W., Wang, G., Gong, L., Shen, Z., Li, C. and Dang, J. (2018), “Research and application of resistance-limiting and energy-dissipating support in large deformation tunnel”, *Chin. J. Rock Mech. Eng.*, **37**(8), 1785-1795. <https://doi.org/10.13722/j.cnki.jrme.2018.0184>.
- Song, F., Wang, H. and Jiang, M. (2018b), “Analytically-based simplified formulas for circular tunnels with two liners in viscoelastic rock under anisotropic initial stresses”, *Constr. Build. Mater.*, **175**, 746-767. <https://doi.org/10.1016/j.apm.2017.10.031>.
- Song, F., Wang, H.N. and Jiang, M.J. (2018a), “Analytical solutions for lined circular tunnels in viscoelastic rock considering various interface”, *Appl. Math. Model.*, **55**, 109-130. <https://doi.org/10.1016/j.apm.2017.10.031>.
- Sulem, J., Panet, M. and Guenot, A. (1987), “An analytical solution for time-dependent displacements in a circular tunnel”, *Int. J. Rock Mech. Min. Sci. Geomech. Abstr.*, **24**(3), 155-164. [https://doi.org/10.1016/0148-9062\(87\)90523-7](https://doi.org/10.1016/0148-9062(87)90523-7).
- Sun, Y., Li, G., Zhang, J. and Qian, D. (2020), “Experimental and numerical investigation on a novel support system for controlling roadway deformation in underground coal mines”, *Energy Sci. Eng.*, **8**(2), 490-500. <https://doi.org/10.1002/ese3.530>.
- Sun, Y., Zhang, J., Li, G., Wang, Y., Sun, J. and Jiang, C. (2019), “Optimized neural network using beetle antennae search for predicting the unconfined compressive strength of jet grouting coalcretes”, *Int. J. Numer. Anal. Meth. Geomech.*, **43**(4), 801-813. <https://doi.org/10.1002/nag.2891>.
- Tian, X., Song, Z. and Wang, J. (2019), “Study on the propagation law of tunnel blasting vibration in stratum and blasting vibration reduction technology”, *Soil Dyn. Earthq. Eng.*, **126**, 105813. <https://doi.org/10.1016/j.soildyn.2019.105813>.
- Tian, X., Song, Z., Wang, B. and Zhou, G. (2020), “A theoretical calculation method of influence radius of settlement based on the slices method in tunnel construction”, *Math. Probl. Eng.*, 5804823. <https://doi.org/10.1155/2020/5804823>.
- Wang, X., Lai, J., He, S., Garnes, R.S. and Zhang, Y. (2020), “Karst geology and mitigation measures for hazards during metro system construction in Wuhan, China”, *Nat. Hazards*, **2020**, 1-23. <https://doi.org/10.1007/s11069-020-04108-3>.
- Wu, K. and Shao, Z. (2019a), “Visco-elastic analysis on the effect of flexible layer on mechanical behavior of tunnels”, *Int. J. Appl. Mech.*, **11**(3), 1950027. <https://doi.org/10.1142/S1758825119500273>.
- Wu, K. and Shao, Z. (2019b), “Study on the effect of flexible layer on support structures of tunnel excavated in viscoelastic rocks”, *J. Eng. Mech.*, **145**(10), 04019077. [https://doi.org/10.1061/\(ASCE\)EM.1943-7889.0001657](https://doi.org/10.1061/(ASCE)EM.1943-7889.0001657).
- Wu, K., Shao, Z. and Qin, S. (2020b), “A solution for squeezing deformation control in tunnels using foamed concrete: A review”, *Constr. Build. Mater.*, **257**, 119539. <https://doi.org/10.1016/j.conbuildmat.2020.119539>.
- Wu, K., Shao, Z. and Qin, S. (2020d), “An analytical design method for ductile support structures in squeezing tunnels”, *Arch. Civ. Mech. Eng.*, **20**(3), 91. <https://doi.org/10.1007/s43452-020-00096-0>.
- Wu, K., Shao, Z., Qin, S. and Li, B. (2020a), “Determination of deformation mechanism and countermeasures in silty clay tunnel”, *J. Perform. Constr. Fac.*, **34**(1), 04019095. [https://doi.org/10.1061/\(ASCE\)CF.1943-5509.0001381](https://doi.org/10.1061/(ASCE)CF.1943-5509.0001381).
- Wu, K., Shao, Z., Qin, S., Zhao, N. and Hu, H. (2020c), “Analytical-based assessment of effect of highly deformable elements on tunnel lining within viscoelastic rocks”, *Int. J. Appl. Mech.*, **12**(3), 2050030. <https://doi.org/10.1142/S1758825120500301>.
- Yuan, Y., Shao, Z., Qiao, R., Fei, X. and Cheng, J. (2020), “Thermal response and crack propagation of mineral components in olivine basalt under microwave irradiation”, *Arab. J. Geosci.*, **13**(14), 589. <https://doi.org/10.1007/s12517-020-05494-5>.

CC